Heptyl mannose decorated glyconanoparticles with tunable morphologies through polymerization induced self-assembly. Synthesis, functionalization and interactions with type 1 piliated E. coli

Xibo Yan, Veronica La Padula, Sabine Favre-Bonté, Julien Bernard

Heptyl Mannose Decorated Glyconanoparticles with Tunable Morphologies through Polymerization Induced Self-Assembly. Synthesis, Functionalization and Interactions with Type 1 Piliated *E coli*

Xibo Yan,[1,*] Veronica La Padula,[2] Sabine Favre-Bonte,[3] Julien Bernard[1,*]

[1]Université de Lyon, Lyon, F-69003, France ; INSA-Lyon, IMP, Villeurbanne, F-69621, France; CNRS, UMR 5223, Ingénierie des Matériaux Polymères, Villeurbanne, F-69621, France.

[2]Centre Technologique des Microstructures (CTμ), Université Claude Bernard Lyon 1, France.

[3]Université de Lyon, France Research Group on "Bacterial Opportunistic Pathogens and Environment". UMR 5557 Ecologie Microbienne, CNRS, Vetagro Sup and Université Lyon1, France.

*Corresponding author

E-mail: xiboyan@hotmail.com (X. Yan) or julien.bernard@insa-lyon.fr (J. Bernard)

ABSTRACT

Mannosylated macro chain transfer agents (MacroCTA) have been used for the RAFT emulsion polymerization of glycidyl methacrylate (GMA) to prepare a series of glyconanoparticles with different morphologies via polymerization-induced self assembly (PISA). Upon increase of PGMA block length and solids content, morphologies progressively evolved from spheres to large vesicles. The epoxide functions located in the core of the nanoparticles were exploited as convenient handles to cross-link the PGMA core and attach red emissive fluorescent tags. Thanks to the presence of multiple *n*-heptyl α-D-mannose ligands on their shell, the glyconanoparticles strongly interacted with type 1 piliated *Escherichia coli* leading to the formation of large bacterial clusters.

Keywords: Glycopolymers, Polymerization-Induced Self-Assembly, Glyconanoparticles, Type 1 piliated *E coli.*

FIGURE FOR ToC_ABSTRACT :

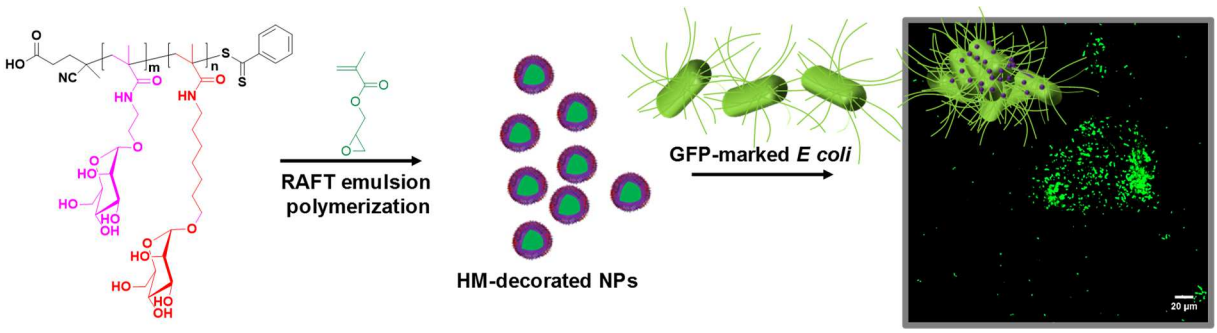

Introduction

Owing to significant advances in macromolecular engineering in the last two decades, glycopolymers have emerged as powerful tools to mimic protein-binding ability of natural carbohydrates, ligands which play a key role in numerous biological processes such as fertilization, cellular communication, apoptosis or host-pathogen interactions.[1-8] Carbohydrate moieties have been incorporated into a large variety of linear, star-shaped, comb-like, dendritic or arborescent macromolecular scaffolds.[9-17] An extensive library of glyconanomaterials, *i.e.* micelles, vesicles or multi-compartment structures, have been generated in a two-step method, where a precisely-defined carbohydrate-containing amphiphilic block copolymer is first prepared and subsequently assembled in a selective solvent (for one of the blocks).[18-22] These glycomaterials find applications in bioimaging and biosensors, targeted drug and gene delivery therapeutic nanomedicine.[23-26]

Under the impetus of Hawkett, Charleux and Pan, Polymerization-Induced Self-Assembly (PISA) has rapidly become a technique of choice to construct organic block copolymer nanoparticles in one step at high solids content and in a scalable fashion.[27-29] The concept of (aqueous) PISA is rather simple and relies on the use of a hydrophilic living polymer precursor which is chain-extended with units of a water-immiscible or water-miscible monomer (emulsion or dispersion polymerizations) leading to the growth of a second block displaying a hydrophobic character. The resulting amphiphilic block copolymers then self-assemble *in situ* in a variety of nanoscale morphologies depending on experimental parameters. Whereas numerous examples of nanoparticles have been described over the last decade using PISA concepts,[30-37] the construction of nanoparticles relying on the use of glycopolymer blocks remains extremely scarce. To our knowledge, the only example of glycopolymer-decorated nanoparticles has been reported by the group of Armes who prepared

a series of biocompatible galactosylated nano-objects (spheres, worms and vesicles) by PISA of 2-hydroxypropyl methacrylate from a binary mixture of macro-CTAs, *i.e.* poly(glycerol monomethacrylate) and a galactose-functionalized polymethacrylate.[38] Relying on turbidimetric lectin binding assays, the authors then demonstrated the capacity of the resulting nano-objects to interact *in vitro* with galectins. Galactosylated vesicles loaded with Rhodamine B octadecyl ester were rapidly internalized by HDF cells and the dye was released intracellularly.

Recently, we reported on the RAFT preparation of precisely-defined glycopolymers bearing multiple pendant copies of n-heptyl α-D-mannose (HM),[39-41] a nanomolar antagonist of FimH.[42] FimH is located at the tip of heteropolymeric fibers, named type 1 pili, expressed by *E coli* bacteria and possesses an adhesive domain with a mannose-binding pocket promoting recognition, attachment of the pathogen to host cells and infection. Thanks to the presentation of multiple sugar residues on their scaffold, HM-functionalized glycopolymers were capable of blocking and disrupting the attachment of bacteria (i.e. adherent invasive *E coli* LF82, a strain involved in bowel inflammatory diseases) to intestinal epithelial cells (*i.e.* T84) *in vitro* at very low concentration (0.1 μM on a mannose unit basis). Anti-adhesive properties of HM-based derivatives were also confirmed in *ex vivo* and *in vivo* conditions.[39-41]

Herein, we extend our previous study and describe the preparation of a variety of HM-decorated nanoparticles using PISA. In a preliminary step, we show that dithiobenzoate-functionalized random copolymers of N-[7-(α-D-mannopyranosyloxy)heptyl] methacrylamide (HMM) and N-[2-(α-D-mannopyranosyloxy)ethyl] methacrylamide (EMM) having adequate molar masses and HMM/EMM compositions can be efficiently employed as macroCTA for the RAFT emulsion polymerization of glycidyl methacrylate (GMA) and for the generation of colloidally stable glyconanoparticles (**Scheme 1**). Then, we demonstrate that

different morphologies are obtained upon precise adjustment of the degree of polymerization for the hydrophobic PGMA block and/or the solids content. To assess the biological activity of HM-functionalized latexes, we finally investigate the capability of P((HMM$_9$-*co*-EMM$_{34}$)-*b*-GMA$_{200}$) mannosylated nanoparticles (spheres, D_z= 70 nm) to interact with type 1 piliated *E. coli*.

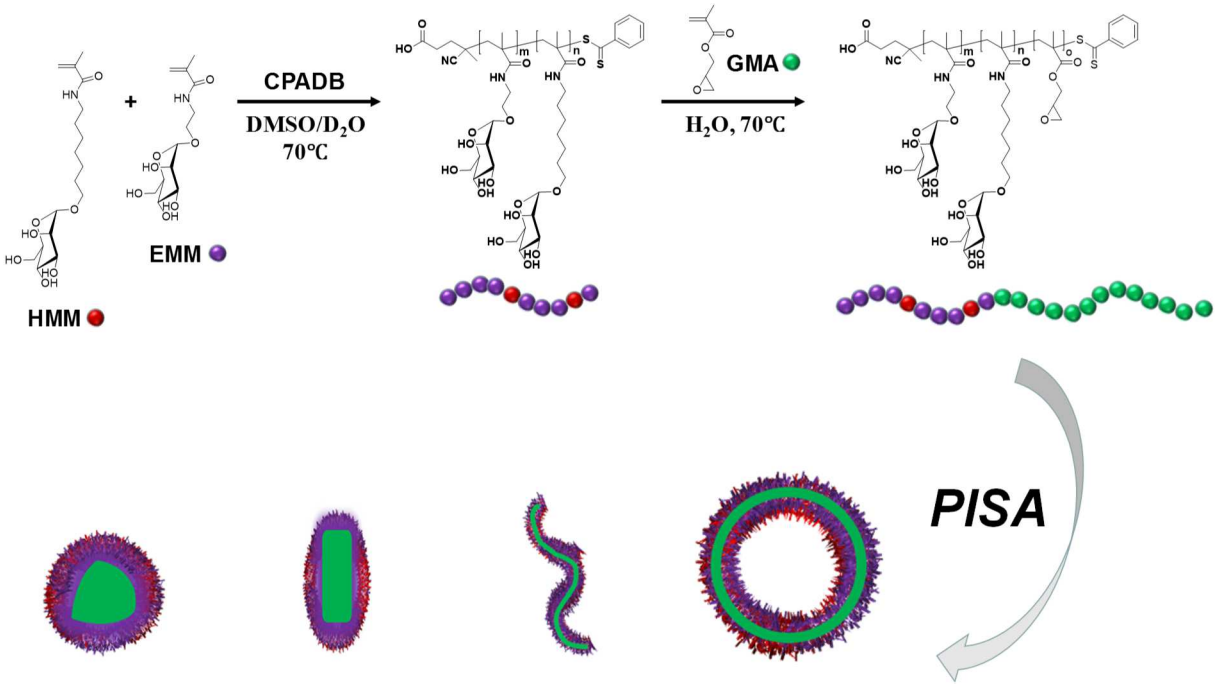

Scheme 1. Route to heptyl mannose decorated glyconanoparticles with tunable morphologies using polymerization-induced self assembly

2. Results and Discussion

In order to generate nano-objects capable to interact with FimH lectin via PISA, we synthesized low molar mass hydrophilic HM-functionalized MacroCTAs. A first macroCTA was prepared by RAFT homopolymerization of N-[7-(α-D-mannopyranosyloxy)heptyl] methacrylamide (HMM) at 70°C in D_2O/DMSO (1/1, v/v) using 4-cyano-4-(phenylcarbonothioylthio) pentanoic acid (CPADB) and 4,4'-azobis(4-cyanovaleric acid) (ACPA) as previously reported ([HMM]$_0$ = 0.37 M and [HMM]$_0$/[CPADB]$_0$/[ACPA]$_0$ =

10/1/0.2).[41,43] Linear pseudo first-order kinetic plots were observed and the resulting homopolymer ($PHMM_9$) exhibited narrow dispersity (Đ<1.10). However, this low molar mass dithiobenzoate-functionalized macroCTA tended to aggregate in water as confirmed by the cloudy appearance of the aqueous glycopolymer solution at 1 mg/mL. Accordingly, chain extension of $PHMM_9$ with GMA in aqueous emulsion conditions ($[GMA]_0/[PHMM_9]_0/[ACPA]_0$=200/1/0.2, T=70°C) resulted in the formation of coagulum even at low solids content (5%). To overcome these colloidal stability issues and preserve the expression of HM moieties at the surface of the nano-objects, a second macroCTA was prepared by RAFT copolymerization of HMM and N-[2-(α-D-mannopyranosyloxy)ethyl] methacrylamide (EMM), a glycomonomer with enhanced solubility in water but without inhibitory activity against AIEC LF82 (at 1 mM on a mannose unit basis).[41] The copolymerization was performed at 70°C in D_2O/DMSO (1/1, v/v) with a $[EMM]_0/[HMM]_0$ ratio equal to 4 and $[HMM]_0$=0.089 M, $([EMM]_0+[HMM]_0)/[CPADB]_0$=50 (see **Table S1**). Again, the copolymerization of HMM and EMM proceeded according to pseudo first-order kinetics and led to the preparation of a copolymer with narrow molar mass distribution ($M_{n,SEC}$=9.2 kg/mol, Đ<1.20). Glycopolymer composition and molar masses P(HMM_9-*co*-EMM_{34}), $M_{n,NMR}$=13.4 kg/mol) were evaluated by ^1H NMR spectroscopy (see **Figure S1**). Aqueous solutions of P(HMM_9-*co*-EMM_{34}) macroCTA were transparent at 1 mg/mL and no formation of large glycopolymer aggregate was detected by Dynamic Light Scattering (D_z = 10 nm in DLS, **Figure S1**).

P(HMM_9-*co*-EMM_{34}) was subsequently chain-extended using glycidyl methacrylate under RAFT aqueous emulsion polymerization conditions (70°C, $[P(HMM_9\text{-}co\text{-}EMM_{34})]_0/[ACPA]_0$=5/1, demineralized water pH=7 as dispersion medium) at different monomer/macroCTA ratios, *i.e.* 200, 400, 600 and 800. The polymerizations were conducted

with solids contents up to 10 wt% owing to the observation of coagulum at higher solids contents.

A

Target composition	Conv. (%)[a]	Solids (% w/w)	$M_{n,SEC}$ ($g.mol^{-1}$)[b]	$Đ^b$
P((HMM$_9$-*co*-EMM$_{34}$)-*b*-GMA$_{200}$)	98	5	11300	1.13
P((HMM$_9$-*co*-EMM$_{34}$)-*b*-GMA$_{200}$)	96	10	10900	1.18
P((HMM$_9$-*co*-EMM$_{34}$)-*b*-GMA$_{400}$)	97	5	16800	1.23
P(HMM$_9$-*co*-EMM$_{34}$)-*b*-GMA$_{400}$)	94	10	15700	1.21
P((HMM$_9$-*co*-EMM$_{34}$)-*b*-GMA$_{600}$)	97	5	21300	1.43
P((HMM$_9$-*co*-EMM$_{34}$)-*b*-GMA$_{800}$)	98	5	26700	1.35

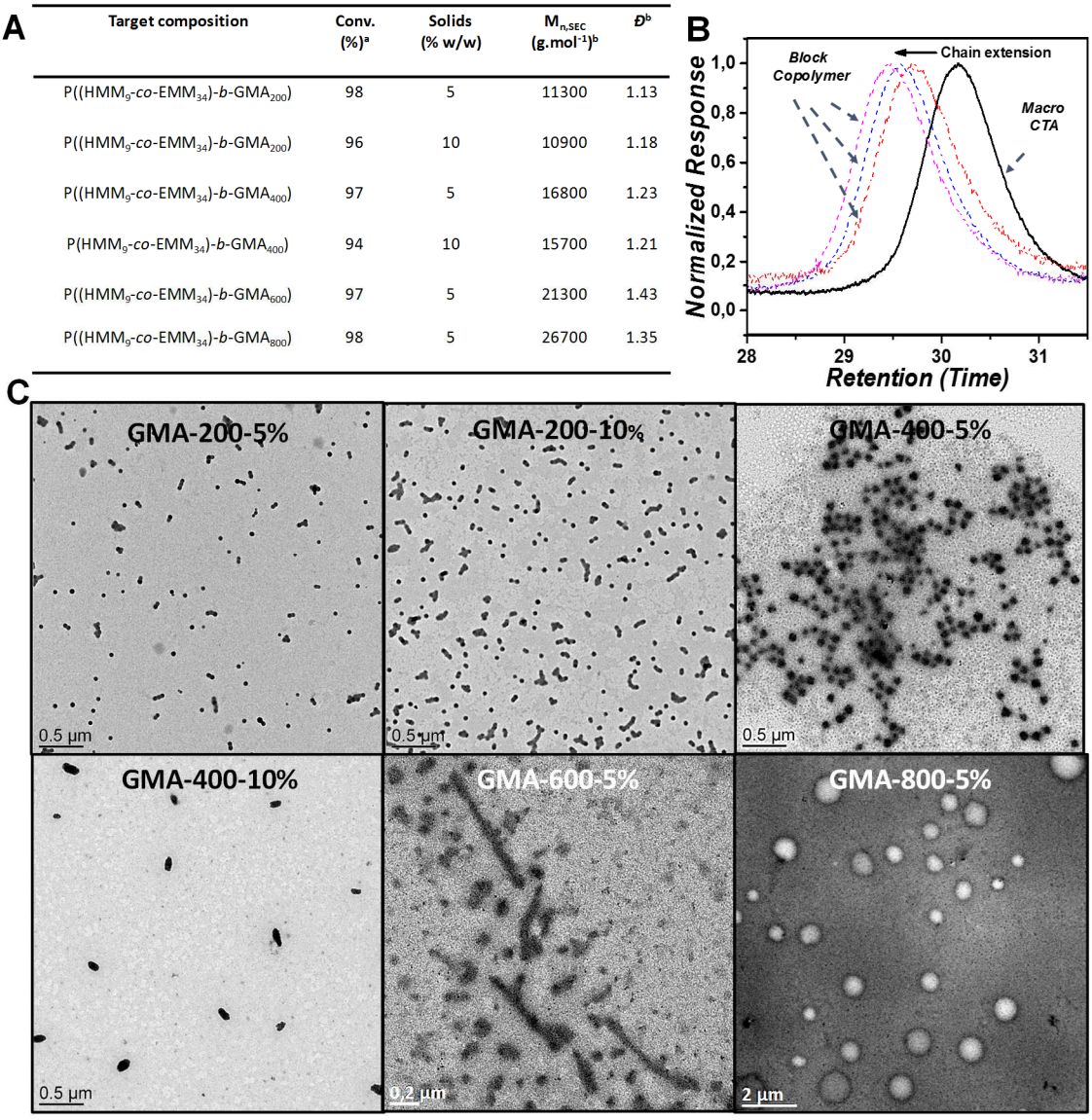

Figure 1. A) Features of P((HMM$_9$-*co*-EMM$_{34}$)-*b*-GMA$_X$) copolymers prepared by RAFT polymerization induced self-assembly in water at 70°C; [a]: Determined by ^{1}H NMR; [b]: Determined by SEC (in THF using PS standards after acetylation of the glycopolymer block); B) Evolution of the SEC traces for P(HMM$_9$-*co*-EMM$_{34}$)-mediated polymerization of GMA at 70°C targeting a DP of 200 and a solid content equal to 5 wt% (analyses in THF using PS standards after acetylation of the glycopolymer block). From right to left, P(HMM$_9$-*co*-EMM$_{34}$) macroCTA and P((HMM$_9$-*co*-EMM$_{34}$)-*b*-GMA$_X$) copolymers at 55% (red), 81%

(blue) and 98% (purple) of GMA conversion. C) TEM images of glyconanoparticles obtained under different conditions of polymerization. GMA-200-5% refers to the P(HMM_9-*co*-EMM_{34})-mediated polymerization of GMA targeting a degree of polymerization of 200 and a solids content of 5% wt.

The kinetics of GMA polymerization at 70°C ($[GMA]_0$=0.25M, $[GMA]_0/[P(HMM_9\text{-}co\text{-}EMM_{34})]_0/[ACPA]_0$=200/1/0.20, 5 wt% solids content) were noticeably slower than the ones reported in other studies dealing with methacrylic monomers[44-45] (see **Figure S2**, ~90% after 8h of reaction *vs* 99% ≥ within 1 or 2h at 50°C and 10 wt% solids content[44]) so that polymerizations were finally stopped after 24h to ensure full conversion of the GMA monomer. As illustrated by **Figure S2**, P(HMM_9-*co*-EMM_{34})-mediated polymerization of GMA proceeded with pseudo-first order kinetics consistent with a constant concentration of radicals. After acetylation of the sugar residues (see experimental details in Supporting Information), the block copolymers were analyzed by SEC in THF using PS calibration. As shown in **Figure 1B**, chain extension of P(HMM_9-*co*-EMM_{34}) with GMA resulted in a progressive shift of the SEC traces (towards lower retention time and thus higher molar mass) as a function of the monomer conversion. In agreement with a good control of the polymerization, SEC traces of the (acetylated) copolymers adopted symmetrical shapes and no low molar mass tailing corresponding to the presence of unreacted macroCTA was detected. Dispersities ranged between 1.10 and 1.25 when degrees of polymerization equal or below 400 were targeted for the PGMA block and increased noticeably (up to 1.43) when longer PGMA blocks were grown (see **Figure 1A**).

The morphologies of the resulting P((HMM_9-*co*-EMM_{34})-*b*-GMA) based nanoparticles were further investigated by TEM and DLS analyses (**Figures 1C** and **S3**). Consistent with the literature, morphologies progressively evolved with the degree of polymerization of the

PGMA block and the solids content. Targeting a degree of polymerization of 200 for the PGMA block afforded narrowly dispersed spherical nanoparticles exhibiting a z-average diameter around 90 nm and a PDI ~0.04 when solids contents were fixed at 5 and 10 wt%. Increasing the length of the hydrophobic PGMA block (Targeted DP ~ 400) either resulted in the construction of spherical nanoparticles (DLS: D_z = 98 nm, PDI=0.05) or rice-shaped nanoparticles (DLS: D_z =121 nm, PDI=0.06. for final solids content equal to 5 and 10 wt%, respectively. In contrast, when the target PGMA degrees of polymerization were 600 and 800, PISA targeting solids contents ~ 5 wt% afforded a mixture of spherical nanoparticles together with short and long worm-like assemblies (two populations observed at 200 nm and 5µm, PDI=0.40) or vesicles (DLS: D_z = 840 nm, PDI=0.26), respectively (**Figure 1C**). Note that DLS of rice-shaped or worm-like particles should be interpreted with caution as the technique reports results as the equivalent spherical diameter which is not relevant for such anisotropic nanoparticles.

Further increase of the solids content to 10% was accompanied by the formation of coagulum in the course of the polymerization when targeting a degree of polymerization superior to 400. The core cross-linking and functionalization of the nano-objects through epoxy-amine reactions was then examined. As epoxides are sensitive to hydrolysis in aqueous medium (especially at high temperatures and/or at acidic or to lesser extent, basic pH),[44,46] we first looked at the stability of the epoxides on the time scale of the polymerization. The copolymers synthesized by PISA (using demineralized water as dispersion medium) were analyzed by ^{1}H NMR spectroscopy in DMSO-d_6 (see spectrum of P((HMM$_9$-*co*-EMM$_{34}$)-*b*-GMA$_{200}$) in **Figure S4**). The characteristic peaks of epoxide rings were clearly identified at 2.66, 2.80 and 3.20 ppm. Comparison of the integrations of the peaks between 7.0 and 8 ppm (belonging to the terminal dithiobenzoate group and amide protons within the glycopolymer block) and at 2.80 and 4.30 ppm suggested that epoxide rings are mostly preserved under

these conditions of polymerization. These functionalities, located within the hydrophobic core of the nano-objects, were then reacted with amines for core cross-linking and functionalization purposes (**Figure 2**). For instance, a degradable water-soluble cross-linker, *i.e.* cystamine (~0.5 eq per epoxide), was incorporated after polymerization ($[GMA]_0/[MacroCTA]_0$ = 200, 5 wt%) at 40°C to stabilize the morphology of the glyconanoparticles. As shown by DLS, the success of the core cross-linking reaction was corroborated by a significant shrinking of nanoparticles diameter in water (D_z decreasing from 92 nm to 70 nm, **Figure 2B**). A similar approach was employed to anchor fluorescent tags onto the nano-objects. Epoxides were then reacted with cystamine (~0.5 eq per epoxide) and Alexa Fluor 555 Cadaverine (AFC, 1 eq. of AFC per copolymer chain) (40°C, 12h, **Figure 2D**). As highlighted by DLS analyses performed after purification by dialysis, concomittant core cross-linking and functionalization of the glyconanoparticles was accompanied by a pronounced decrease of the z-average diameter (D_z = 71 nm, PDI=0.09, **Figure S5**). Consistent with the ligation of AFC within the core of the nanoparticles, the resulting dispersion (purified by dialysis) exhibited a fluorescence emission at 566 nm (**Figure 2D**).

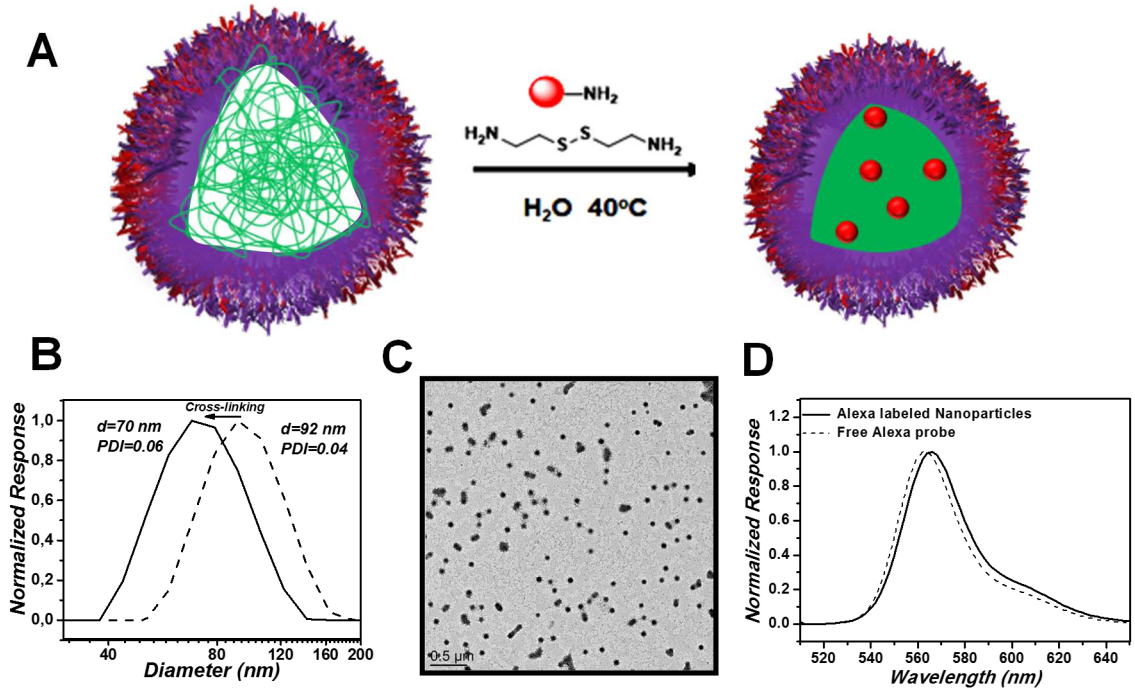

Figure 2. A) Schematic illustration of core-cross-linking and functionalization of glyconanoparticles through epoxy-amine reaction; B) Size evolution before and after core-cross-linking of the P((HMM$_9$-*co*-EMM$_{34}$)-*b*-GMA$_{200}$) glyconanoparticles as measured by DLS; C) TEM image of core-cross-linked AFC-labeled P((HMM$_9$-*co*-EMM$_{34}$)-*b*-GMA$_{200}$) glyconanoparticles; D) Fluorescence emission spectrum of AFC-labeled P((HMM$_9$-*co*-EMM$_{34}$)-*b*-GMA$_{200}$) glyconanoparticles.

Finally, we investigated the ability of n-heptyl α-D-mannose decorated nanoparticles to interact with green fluorescent protein labeled AIEC LF82 strains using confocal fluorescence microscopy. In the absence of glyconanoparticles, AIEC LF82 bacteria ($OD_{620\ nm}$ = 0.6, fluorescence emission at 520 nm) did not agglomerate after 24 hours of incubation. In contrast, incubation of spherical P(HMM$_9$-*co*-EMM$_{34}$)-*b*-GMA$_{200}$) glyconanoparticles with AIEC LF82 (for 12 hours) resulted in the agglutination of the bacteria (see **Figure 3B**). Careful examination of **Figures 3B** and **3C** (see also overlapped images in **Figure S6**) confirmed that red emitting AFC-decorated glyconanoparticles accumulate on *E. coli* thanks to the presentation of multiple HM residues at their surface, and promote the formation of very large clusters (~ 100 µm).

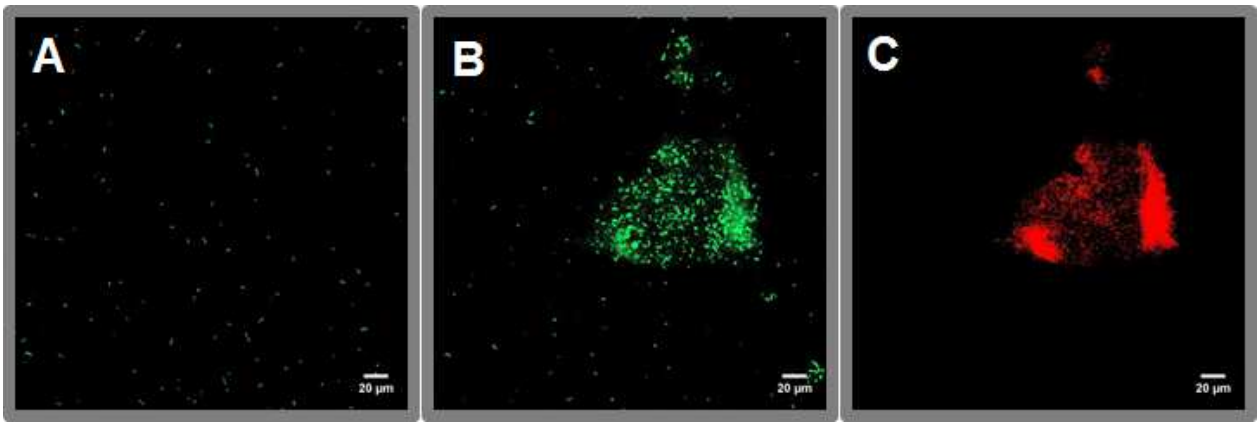

Figure 3. Confocal fluorescence microscopy pictures of A) GFP marked AIEC LF82 after 24h of incubation (blank experiment); B) and C) bacterial clusters observed after co-incubation of

GFP-marked AIEC LF82 and AFC-labeled P((HMM$_9$-*co*-EMM$_{34}$)-*b*-GMA$_{200}$) glyconanoparticles for 12h (λ_{exc} = 488 nm for GFP and 543 nm for AFC).

3. Conclusions

In conclusion, a library of HM-decorated glyconanomaterials with tunable morphologies (spheres, rice-shaped nanoparticles, vesicles) have been synthesized by polymerization induced self assembly. The presence of epoxide rings offered a convenient platform for stabilization or/and functionalization of resulting glyconanomaterials. Thanks to the strong binding affinity of HM residues with FimH adhesin, the multivalent glyconanoparticles were shown to interact with type 1 piliated *E coli* as confirmed by the rapid aggregation of the pathogens. These model HM-functionalized nanoparticles are expected to open new perspectives for the targeted delivery of antimicrobial or anti-inflammatory agents.

Supporting Information

Supporting Information is available.

Conflicts of interest

The authors declare no competing financial interest.

Acknowledgements:

The authors thank Centre Technologique des Microstructures (CTμ) for their help with the TEM microscopy. We express thanks to the group of Pr Nicolas Barnich (Clermont Université, UMR 1071, Inserm/Université d'Auvergne, 63000 Clermont-Ferrand, France) for

providing the AIEC reference strain LF82. We thank the French Agency for National Research (ANR) for funding X.Y. post-doc (PREPROPOSAL, ANR-15-CE09-0021).

References

[1] R. A. Dwek, Glycobiology: Toward Understanding the Function of Sugars, Chemical Reviews 96 (1996), 683-720.

[2] C. R. Bertozzi, L. L. Kiessling, Chemical glycobiology, Science 291 (2001), 2357-2364.

[3] S. Akira, S. Uematsu, O. Takeuchi, Pathogen recognition and innate immunity, Cell 124 (2006), 783-801.

[4] P. Poignard, E. O. Saphire, P. Parren, D. R. Burton, GP120: Biologic Aspects of Structural Features, Annual Review of Immunology 19 (2001), 253-274.

[5] M. Ambrosi, N. R. Cameron, B. G. Davis, Lectins: tools for the molecular understanding of the glycocode, Organic & Biomolecular Chemistry 3 (2005), 1593-1608.

[6] K. T. Pilobello, L. K. Mahal, Deciphering the glycocode: the complexity and analytical challenge of glycomics, Current Opinion in Chemical Biology 11 (2007), 300-305.

[7] S. R. Simon Ting, G. Chen,M. H. Stenzel, Synthesis of glycopolymers and their multivalent recognitions with lectins, Polym. Chem. 1 (2010), 1392-1412.

[8] S. G. Gouin, Multivalent Inhibitors for Carbohydrate-Processing Enzymes: Beyond the "Lock-and-Key" Concept, Chem. Eur. J. 20 (2014), 11616-11628.

[9] J. Geng, G. Mantovani, L. Tao, J. Nicolas, G. J. Chen, R. Wallis, D. A. Mitchell, B. R. G. Johnson, S. D. Evans, D. M. Haddleton, Site-directed conjugation of "clicked" glycopolymers to form glycoprotein mimics: binding to mammalian lectin and induction of immunological function, Journal of the American Chemical Society 129 (2007), 15156-15163.

[10] Y. Abdouni, G. Yilmaz, C. R. Becer, Sequence and Architectural Control in Glycopolymer Synthesis, Macromolecular Rapid Communications 38 (2017), 1700212.

[11] W. Qi, Y. Zhang, J. Wang, G. Tao, L. Wu, Z. Kochovski, H. Gao, G. Chen, M. Jiang, Deprotection-Induced Morphology Transition and Immunoactivation of Glycovesicles: A Strategy of Smart Delivery Polymersomes, J. Am. Chem. Soc. 140 (2018), 8851-8857.

[12] J. Bernard, X. Hao, T. P. Davis, C. Barner-Kowollik, M. H. Stenzel, Synthesis of Various Glycopolymer Architectures via RAFT Polymerization: From Block Copolymers to Stars, Biomacromolecules 7 (2006), 232-238.

[13] A. Dag, J. Zhao, M. H. Stenzel, Origami with ABC Triblock Terpolymers Based on Glycopolymers: Creation of Virus-Like Morphologies, ACS Macro Lett. 4 (2015), 579-583.

[14] H. Al-Mughaid, and T. B. Grindley, Synthesis of a Nonavalent Mannoside Glycodendrimer Based on Pentaerythritol, J. Org. Chem. 71 (2006), 1390-1398.

[15] M. Semsarilar, V. Ladmiral, S. Perrier, Highly Branched and Hyperbranched Glycopolymers via Reversible Addition–Fragmentation Chain Transfer Polymerization and Click Chemistry, Macromolecules 43 (2010), 1438-1443.

[16] J. Bernard, M. Schappacher, A. Deffieux, M-H. Charles, M-T. Charreyre, T. Delair, P. Viville, R. Lazzaroni, Water-Soluble Dendrigrafts Bearing Saccharidic Moieties: Elaboration and Application to Enzyme Linked OligoSorbent Assay (ELOSA) Diagnostic Tests, Bioconjugate Chem. 17 (2006), 6-14.

[17] A. Guerry; S. Cottaz; E. Fleury; J. Bernard; S. Halila. Redox-stimuli responsive micelles from DOX-encapsulating polycaprolactone-g-chitosan oligosaccharide, Carbohydrate Polymers 112 (2014), 746-752.

[18] S. de Medeiros Modolon, I. Otsuka, S. Fort, E. Minatti, R. Borsali, S. Halila, Sweet Block Copolymer Nanoparticles: Preparation and Self-Assembly of Fully Oligosaccharide-Based Amphiphile, Biomacromolecules 13 (2012), 1129-1135.

[19] C. Bonduelle; H. Oliveira; C. Gauche; J. Huang; A. Heise; S. Lecommandoux, Multivalent effect of glycopolypeptide based nanoparticles for galectin binding, Chemical Communications 52 (2016), 11251-11254.

[20] J. Zhao; H. Lu, P. Xiao, M. H. Stenzel, Cellular Uptake and Movement in 2D and 3D Multicellular Breast Cancer Models of Fructose-Based Cylindrical Micelles That Is Dependent on the Rod Length, ACS Appl. Mater. Interfaces 8 (2016), 16622-16630.

[21] L. Su, C. Wang, F. Polzer, Y. Lu, G. Chen, M. Jiang, Glyco-Inside Micelles and Vesicles Directed by Protection–Deprotection Chemistry, ACS Macro Lett. 3 (2014), 534-539.

[22] Q. Guo; T. Zhang; J. An; Z. Wu; Y. Zhao; X. Dai; X. Zhang; C. Li, Block versus Random Amphiphilic Glycopolymer Nanopaticles as Glucose-Responsive Vehicles, Biomacromolecules 16 (2015), 3345-3356.

[23] X. Wang, O. Ramstrom, M. D. Yan, Glyconanomaterials: Synthesis, Characterization, and Ligand Presentation, Advanced Materials 22 (2010), 1946-1953.

[24] N. C. Reichardt, M. Martin-Lomas, S. Penades, Opportunities for glyconanomaterials in personalized medicine, Chemical Communications 52 (2016), 13430−13439.

[25] O. Ramstrom, M. D. Yan, Glyconanomaterials for Combating Bacterial Infections, Chemistry-A European Journal 21 (2015), 16310-16317.

[26] N. J. Hao, K. Neranon, O. Ramstrom, M. D. Yan, Glyconanomaterials for biosensing applications, Biosensors & Bioelectronics 76 (2016), 113-130.

[27] C. J. Ferguson, R. J. Hughes, B. T. T. Pham, B. S. Hawkett, R. G. Gilbert, A. K. Serelis, C. H.Such, Effective ab Initio Emulsion Polymerization under RAFT Control, Macromolecules 25 (2002), 9243-9245.

[28] W. Wan, C. Hong, C. Pan, One-pot synthesis of nanomaterials via RAFT polymerization induced self-assembly and morphology transition, Chem. Commun. 39 (2009), 5883–5885.

[29] G. Delaittre, C. Dire, J. Rieger, J.-L. Putaux, B. Charleux, Formation of polymer vesicles by simultaneous chain growth and self-assembly of amphiphilic block copolymers, Chem. Commun. 20 (2009), 2887−2889.

[30] Y. Deng, C. Yang, C. Yuan, Y. Xu, J. Bernard, L. Dai, J-F. Gérard, Hybrid organic–inorganic block copolymer nano-objects from RAFT polymerization-induced self-assembly, J. Polym. Sci. Part A 51 (2013), 4558-4564.

[31] Y. Ding, M. Cai, Z. Cui, L. Huang, L. Wang, X. Lu, Y. Cai, Synthesis of Low‐Dimensional Polyion Complex Nanomaterials via Polymerization‐Induced Electrostatic Self‐Assembly, Angew. Chem. Int. Ed. 57 (2018), 1053-1056.

[32] X. Chen, L. Liu, M. Huo, M. Zeng, L. Peng, A. Feng, X. Wang, J. Yuan, Direct Synthesis of Polymer Nanotubes by Aqueous Dispersion Polymerization of a Cyclodextrin/Styrene Complex, Angew. Chem. Int. Ed. 56 (2017), 16541-16545.

[33] Q. Xu, T. Huang, S. Li, K. Li, C. Li, Y. Liu, Y. Wang, C. Yu, Y. Zhou, Emulsion-Assisted Polymerization-Induced Hierarchical Self-Assembly of Giant Sea Urchin-like Aggregates on a Large Scale, Angew. Chem. Int. Ed. 57 (2018), 8043-8047.

[34] X. Wang, J. Zhou, X. Lv, B. Zhang, Z. An, Temperature-Induced Morphological Transitions of Poly(dimethylacrylamide)-Poly(diacetone acrylamide) Block Copolymer Lamellae Synthesized via Aqueous Polymerization-Induced Self-Assembly, Macromolecules 50 (2017), 7222-7232.

[35] J. Yeow, C. Boyer, Photoinitiated Polymerization-Induced Self-Assembly (Photo-PISA): New Insights and Opportunities, Advanced Science 133 (2017), 1700137.

[36] X. G. Qiao; O. Lambert; J.-C. Taveau; P.-Y. Dugas; B. Charleux; M. Lansalot; E. Bourgeat-Lami, Nitroxide-Mediated Polymerization-Induced Self-Assembly of Block Copolymers at the Surface of Silica Particles: Toward New Hybrid Morphologies, Macromolecules 50 (2017), 3796-3806.

[37] G. Mellot; P. Beaunier; J-M. Guigner; L. Bouteiller; J. Rieger; F. Stoffelbach, Beyond Simple AB Diblock Copolymers: Application of Bifunctional and Trifunctional RAFT Agents to PISA in Water, Macromol. Rapid Commun. 1800315.

[38] V. Ladmiral, M. Semsarilar, I. Canton, S. P. Armes, Polymerization -Induced Self-Assembly of Galactose-Functionalized Biocompatible Diblock Copolymers for Intracellular Delivery, Journal of the American Chemical Society 2013, 135, 13574-13581.

[39] X. Yan, A. Sivignon, P. Alcouffe, B. Burdin, S. Favre-Bonte, R. Bilyy, N. Barnich, E. Fleury, F. Ganachaud, J. Bernard, Brilliant Glyconanocapsules for Trapping of Bacteria, Chem. Commun. 51 (2015), 13193-13196.

[40] X. Yan, A. Sivignon, N. Yamakawa, A. Crepet, C. Travelet, R. Borsali, T. Dumych, Z. L. Li, R. Bilyy, D. Deniaud, E. Feury, N. Barnich, A. Darfeuille-Michaud, S. G. Gouin, J. Bouckaert, J. Bernard, Glycopolymers as Antiadhesives of E. coli Strains Inducing Inflammatory Bowel Diseases, Biomacromolecules 16 (2015), 1827-1836.

[41] A. Sivignon, X. Yan, D. Alvarez Dorta, R. Bonnet, J. Bouckaert, E. Fleury, J. Bernard, S. G. Gouin, A. Darfeuille-Michaud, N. Barnich, Development of Heptylmannoside-Based Glycoconjugate Antiadhesive Compounds against Adherent-Invasive Escherichia coli Bacteria Associated with Crohn's Disease, mBio 6 (2015), 6 e01298-15.

[42] J. Bouckaert, J. Berglund, M. Schembri, E. De Genst, L. Cools, M. Wuhrer, C. S. Hung, J. Pinkner, R. Slattegard, A. Zavialov, D. Choudhury, S. Langermann, S. J. Hultgren, L. Wyns, P. Klemm, S. Oscarson, S. D. Knight, H. De Greve, Receptor binding studies disclose a novel class of high-affinity inhibitors of the Escherichia coli FimH adhesin, Molecular Microbiology 55 (2005), 441-455.

[43] X. Yan, M. Delgado, A. Fu, P. Alcouffe, S. G. Gouin, E. Fleury, J. L. Katz, F. Ganachaud, J. Bernard, Simple but Precise Engineering of Functional Nanocapsules through Nanoprecipitation, Angewandte Chemie-International Edition 53 (2014), 6910-6913.

[44] F. L. Hatton, J. R. Lovett, S. P. Armes, Synthesis of well-defined epoxy-functional spherical nanoparticles by RAFT aqueous emulsion polymerization, Polym. Chem. 8 (2017), 4856-4868.

[45] J. Tan; D. Liu; C. Huang; X. Li; J. He; Q. Xu; L. Zhang, Photoinitiated Polymerization‐Induced Self‐Assembly of Glycidyl Methacrylate for the Synthesis of Epoxy‐Functionalized Block Copolymer Nano‐Objects, Macromol. Rapid. Commun. 38 (2017), 1700195.

[46] Pauline Sallet, PhD Thesis, INSA de Lyon, 2017.

Graphical abstract